

Article

Effects of Residue Cover on Infiltration Process of the Black Soil Under Rainfall Simulations

Yan Xin, Yun Xie * and Yuxin Liu

State Key Laboratory of Earth Surface Processes and Resource Ecology, Faculty of Geographical Science, Beijing Normal University, Beijing 100875, China; xinyanhao51@163.com (Y.X.); day_dream_lyx@163.com (Y.L.)

* Correspondence: xieyun@bnu.edu.cn; Tel.: +86-10-5880-7391

Received: 19 September 2019; Accepted: 5 December 2019; Published: 9 December 2019



Abstract: Residue cover is widely used for soil conservation after crop harvesting in the black soil region of the Northeastern China, which influences infiltration. It is necessary to optimize infiltration models for accurate predictions under bare and residue cover slope conditions. Rainfall simulation experiments were conducted to quantify the infiltration for the black soil under four rainfall intensities (30, 60, 90, and 120 mm/h), five residue coverage controls (15%, 35%, 55%, 75%, and bare slope), and two soil moisture (8% and approximately 30%) conditions. The observed data were used to fit and compare four infiltration models by Kostiakov, Mein and Larson (short for GAML, a modification of GreenAmpt model made by Mein and Larson), Horton, and Philip under the bare slope conditions. The residue cover infiltration factor (RCF_i) was derived to predict the infiltration under the residue cover slopes, which was defined as the ratio of infiltration from residue-covered soil to that from bare soil. The results showed that the newly derived equation coupling the Philip model with the RCF_i was the most accurate way of predicting the cumulative infiltration of black soil under various residue covers, and could be applied to the black soil region for residue cover infiltration predictions.

Keywords: infiltration estimation; black soil; residue cover; model validation

1. Introduction

Infiltration is the process of water entering soil from the soil surface [1,2]. This process is one of the most important components in the hydrological cycle and is related to many environmental problems and soil erosion [3]. It is influenced by many internal and external factors, such as rainfall characteristics, slope gradients, soil hydraulic properties, soil properties, and surface sealing, which makes infiltration hard to quantify [4].

Numerous models have been proposed for vertically homogeneous soils with constant initial soil water content and flow over horizontal surfaces for infiltration estimations [5,6], including physically-based models and empirical models [7–14]. However, these models have limited applicability under complex initial factors. Many studies have been conducted to modify the applications of these models under various scenarios and assumptions. The Green–Ampt model is one of the most widely used hydrological and erosion models, as it involves simple expression, uses few parameters, and has a specific physical meaning. The model was initially developed to simulate infiltration under ponding conditions in homogeneous soil [15]. Modifications have continuously been proposed to expand the scope of the model's application so that infiltration can be simulated under steady rainfall events [16], layered soil [17], or unsaturated soil with different slopes [18–20], as well as other conditions. The aforementioned models should be modified and improved based on a variety of scenarios to obtain the most accurate infiltration estimations.

Black soil, classified as a Haplic-Ustic somuosol in the Chinese Soil Taxonomy and Udic Argiboroll in the U.S. Soil Taxonomy [21], is mainly distributed in Northeastern China. As this soil is rich in

organic matter (OM) and appears black, it is referred to as “black soil” and the “black soil region” by local people and researchers alike [22]. The parent material of the soil contains mostly loess clay loam deposits. Due to the fine soil texture, black soil is poor in terms of permeability and is easily eroded. Coupled with the effect of seasonal variation in the region, i.e., freeze–thaw erosion in the winter and spring and rainstorm erosion in the flood season, black soil is impacted by severe runoff erosion. Erosion diminishes the OM content and soil thickness, and even induces decreasing soil productivity and environmental deterioration. It is essential to study black soil infiltration processes to prevent soil erosion.

Leaving field residues on the top of soil is a practical conservation tillage in the black soil region since there is a large annual production of crop residues. It was demonstrated that residue cover had a positive effect on soil infiltration, which increased infiltration into the soil and reduced surface runoff [19]. Although, researchers have paid much attention to the benefits of residue cover in terms of preserving soil and water and maintaining soil productivity, they have so far neglected infiltration estimation under residue cover [22,23]. Moreover, infiltration models have been mostly used for bare soils without the effects of residue cover. It is therefore necessary to modify the existing infiltration models to take into account the effects of residue cover for infiltration estimations of black soil on farmland.

In this study, the infiltration process of black soil under various rainfall intensities and residue coverages was studied with simulated rainfall. The objectives of the paper are:

- (1) To determine the optimal infiltration model for bare black soil;
- (2) To establish the infiltration model combined with the effect of residue cover for black soil.

2. Materials and Methods

2.1. Design of Rainfall Simulation Experiments

Rainfall simulation experiments were conducted to study infiltration using spray-nozzle rainfall simulators and soil flumes in the rainfall simulation laboratory of Beijing Normal University, China, in 2015 (Figure 1). Four levels of rainfall intensities (including 30, 60, 90, and 120 mm/h), two soil moistures (8% and 30%, measured by TDR soil moisture sensor (Time domain reflectometry, CAMPBELL TDR200, Campbell Scientific, Inc., U.S.), representing the extremely dry and extremely wet runs), and 7% slope (defined as “intense erosion”, according to the grade scale of soil erosion intensity standard in the experimental field) were designed for the laboratory experiments. Five residue coverages (15%, 35%, 55%, 75%, and bare slope as a control), determined by the digital photograph method, were designed to quantify the residue cover effect. Corn stalks were collected to use in the experiments. Each rainfall event was performed in both dry and wet runs and lasted for 1 h under various rainfall intensities. The interval was 24 h between runs. In total, 80 runs were conducted. All treatments were performed twice for reproducibility and precision.

The experimental black soil used was the top 20 cm of surface soil from farmland and classified by light erosion intensity, collected from the Jiusan Soil Conservation Station. The characteristics of the black soil included an organic matter content of 5.0% and a particle size distribution of 32%, 33%, and 35% for sand, silt, and clay, respectively. The soil was filled into the flume with a depth of 0.25 m (2 m length \times 1 m width \times 0.35 m depth) and layered with a soil density of 1.07 to 1.25 g/cm³ to model actual field conditions. The upper soil layer was 0.1 m deep and the sublayer was 0.15 m deep, and the contact surface of the two layers was roughened to reduce soil stratification which could affect infiltration [24]. A wooden board was used for the soil surface flattening to reduce the effect of soil roughness.

The precipitation of each rainfall event was controlled by simulators. The runoff was collected into bottles for measurement every 5 min during rainfall, and volumes were recorded after the rain. The infiltration amount was the difference between the rainfall amount and the runoff; evaporation

and residue retention during the rainfall events were not measured. The infiltration data obtained were used to determine the hydrological parameters in the models.



Figure 1. Laboratory experimental setup.

2.2. The Residue Cover Factor for Model Validation

Once the optimal infiltration model was determined for the bare soil, the infiltration under the residue cover could be predicted using a ratio multiplying the function of the bare soil, according to Xin et al. [25]. Therefore, the optimal infiltration model under the residue cover was

$$f(i, t)_r = RCF_i \times f(i, t)_b, \quad (1)$$

where $f(i, t)_r$ is the infiltration model under residue cover (mm/min), i is the infiltration rate (mm/min), t is the corresponding time (min), RCF_i is the residue cover factor, and $f(i, t)_b$ is the optimal infiltration model of the bare soil. RCF_i is the ratio of infiltration amounts from the residue cover soil and the bare soil, which was described as

$$RCF_i = CI_r / CI_b, \quad (2)$$

where CI_r and CI_b are the cumulative infiltration amount (mm) of the residue cover and bare soil under the rainfall events, respectively. The relationship between the residue cover infiltration factor (RCF_i) and residue cover was established as

$$RCF_i = 0.94 \times RC + 1, \quad (3)$$

where RC is the residue cover (Figure 2).

The performances of four common infiltration models were compared to evaluate the bare black soil infiltration, including Kostiakov [8], Horton [9], Philip [11], and Mein and Larson (GAML) models (Table 1). The infiltration models were different in terms of mathematical structure and hydrological parameters, but their estimates were all based on the measured water infiltration data for bare soil conditions [26].

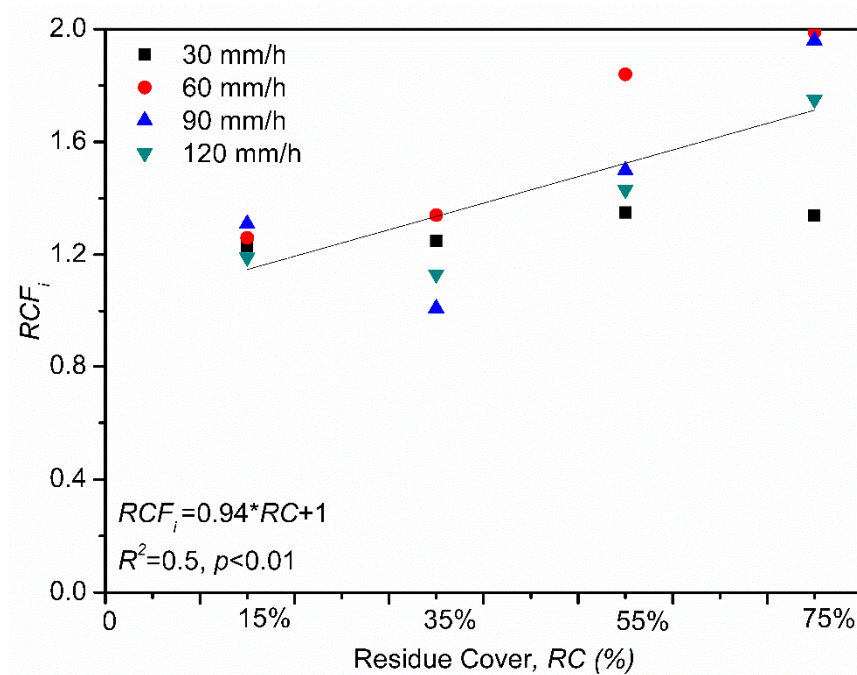


Figure 2. The relationship between the residue cover infiltration factor (RCF_i) to predict the infiltration and the residue cover.

Table 1. The four infiltration models.

Model	Year	Equation	Symbols
Kostiakov [8]	1932	$f(t) = Bt^{-n}$	B , fitting parameters
Horton [9]	1933	$f(t) = f_c + (f_0 - f_c)e^{-kt}$	f_0 , initial rate f_c , constant rate k , decay constant
Philip [11]	1957	$f(t) = 0.5St^{-0.5} + K_s$	S , sorptivity K_s , saturated hydraulic conductivity
Mein and Larson (GAML) [16]	1973	$f(t) = K_e \left(\frac{1+S \cdot M}{F} \right)$	F , cumulative infiltration K_e , effective hydraulic conductivity S , suction at the wetting front M , hydrological parameter of difference between saturated and initial volumetric moisture content

Note: $f(t)$ is the infiltration rate and t represents the time.

2.3. Accuracy Assessment Methods

Nonlinear regression was used to determine the values of the parameters in the infiltration models with the rainfall data under the bare soil. The observed values beneath the residue cover and the corresponding predicted values were compared to evaluate the simulations of the models using the 1:1 line method. This method pertains to the t-test method to estimate whether the confidence interval of the slope and intercept of the regressed equation included the numbers 1 and 0, respectively [25]. If included, no difference existed between the regressed curve and the 1:1 line.

The root mean square error (RMSE), the Nash–Sutcliffe efficiency (NSE), and the determination coefficient (R^2) were used to evaluate the accuracy of the infiltration models [27,28]. The equations of the statistical indexes were as follows:

$$RMSE = \sqrt{\frac{\sum_{i=1}^N (Y_i - O_i)^2}{N}}, \quad (4)$$

$$NSE = 1 - \frac{\sum_{i=1}^N (Y_i - O_i)^2}{\sum_{i=1}^N (O_i - \bar{O}_i)^2}, \quad (5)$$

$$R^2 = \frac{\sum_{i=1}^N (Y_i - \bar{O}_i)^2}{\sum_{i=1}^N (O_i - \bar{O}_i)^2}, \quad (6)$$

where O_i is the i th observed value, \bar{O}_i is the average observed value of all of the observed events, Y_i is the i th predicted value, and N is the total number of events. The higher the NSE values were, the better the model performed, as it represented the level of agreement between the observed and predicted values [29]. The values of the RMSE showed the opposite result, namely, the lower the RMSE values were, the better the model performed. The closer to 1 the determination coefficient R^2 was, the higher the correlation was. The range of the values of R^2 was 0–1, while the range of the values of NSE was $(-\infty)$ –1. In the present study, O_i represented the observed values and Y_i represented the predicted values of the infiltration rates.

3. Results

3.1. Infiltration Rates of Bare Black Soil Under Various Rainfall Events

The average values of two repeated trials were used for the infiltration rate curves for different rainfall intensities and soil moistures of the black soil (Figure 3). The initial infiltration rates were equal to the rainfall intensities before ponding. When the water ponded on the surface, infiltration occurred at the potential infiltration rate and runoff generation began. The times to runoff in the dry runs were around 48.0, 16.0, 7.4, and 5.1 min, and the total infiltration amounts were 27.67, 38.30, 45.14, and 47.54 mm under the four rainfall intensities, respectively. The higher the rainfall intensities were, the earlier the runoff began. Then, infiltration rates decreased and tended to become steady as the rainfall continued due to the soil crust that formed on the soil surface. The final infiltration rates of the dry runs were 0.37, 0.40, 0.53, and 0.54 mm/min. In contrast, the runoff times of the wet runs were within 5 min and the infiltration rate became stable soon after runoff generation under various rainfall intensities. The final infiltration rates corresponding to the rainfall intensities were 0.21, 0.23, 0.43, and 0.51 mm/min, respectively. The total infiltration amounts were 44.43, 55.05, 72.81, and 80.18 mm under the four rainfall intensities.

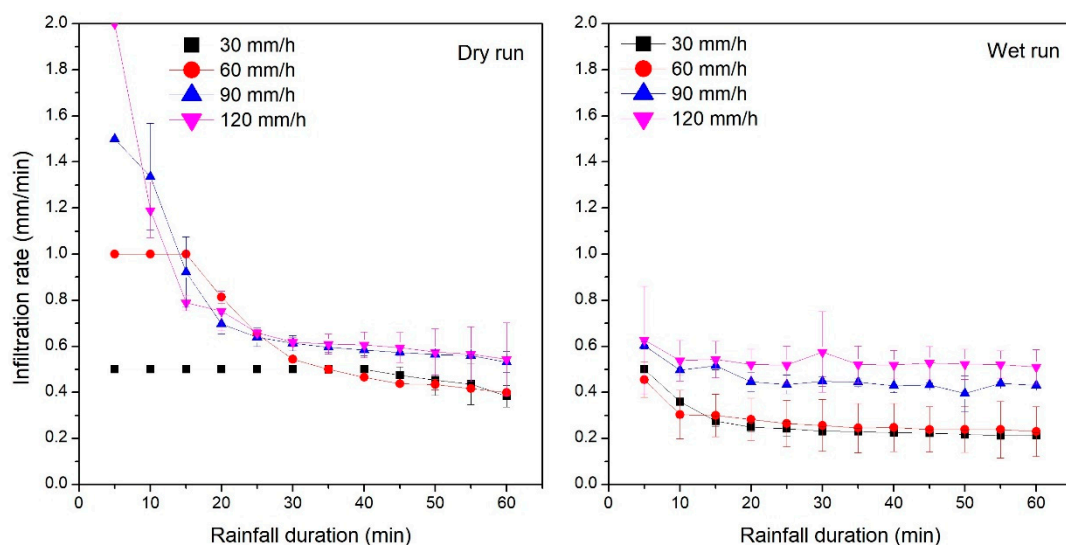


Figure 3. Infiltration rates under various rainfall events.

3.2. Estimation of the Infiltration Model Parameters

The infiltration rates under the various rainfall intensities on the bare soil were used to fit the four models. The values of each parameter were regressed; these are listed in Table 2. As shown, the S-M parameter in the GAML model was negative (equal to -0.572), which was an invalid value. Therefore, the other three models were used for the infiltration estimation of the black soil, but not the GAML model. The determination coefficient R^2 was approximately 0.5, and the regression results passed the significance test at the $p = 0.01$ level.

Table 2. The fitted parameters of different infiltration models.

Kostiakov				Horton			Philip			GAML			
B	n	R^2	f_c	f_0	k	R^2	S	K_s	R^2	K_e	$S \cdot M$	R^2	
1.511	0.352	0.494	0.421	1.199	0.096	0.511	3.185	0.290	0.509	0.507	-0.572	0.553	

3.3. Cumulative Infiltration Amounts for the Residue-Covered Black Soil under Various Rainfall Events

The cumulative infiltration amounts of the residue cover on the black soil under different rainfall events are shown in Figure 4. It was indicated that the residue cover tillage was effective at promoting the infiltration of the black soil and delaying the runoff generation. Under the 30 mm/h scenario, the precipitation nearly seeped into the soil when the residue cover was more than 55%, which proved that the tillage was effective under the relatively small rainfall intensity events. The infiltration amounts did not show that the higher the residue coverages were, the higher the infiltration amounts were. The infiltration amounts under 35% residue cover were less than under 15% residue cover. This result might have been due to the fixed runoff flow path, which could have promoted runoff generation [30].

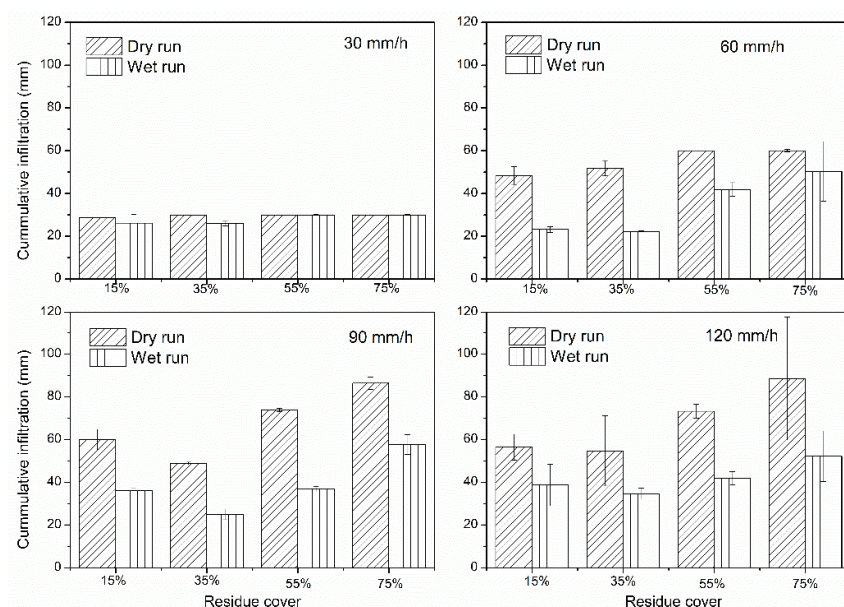


Figure 4. Cumulative infiltration amounts under various rainfall events.

3.4. Performance of the Models for the Residue-Covered Black Soil

According to Xin et al. [25], RCF_i was used to fit the infiltration rates of the residue-covered black soil. The performances of the three models were evaluated and the results showed that the Kostiakov model performed poorly. As it did not pass the 1:1 line test for the confidence interval of the slope and intercept of the regressed equation, excluding the numbers 1 and 0, respectively. The Horton and Philip models performed well (Figure 5). As is generally accepted, the performance of the Kostiakov model was robust for many soils over short time periods [31]. In our study, the performance of this model

was good for the bare black soil, but it did not perform well after adding the effects of the residue cover in the multiplication form (Equation (1)). The multiplication form underestimated the initial infiltration rate under the high residue coverage scenario, which was in accordance with Almeida et al. [32] who used the Kostiakov–Lewis model for estimation, with the results indicating that the Kostiakov–Lewis model underestimated the infiltration rates at the beginning of the rainfall event and overestimated the rates at the end of the rainfall.

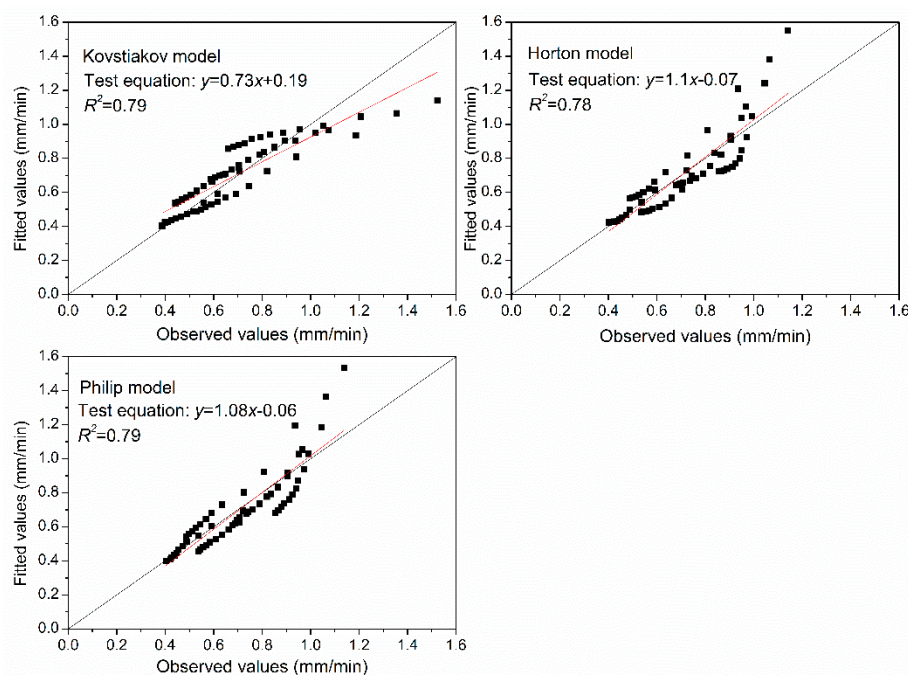


Figure 5. Comparison of the observed and fitted infiltration rates obtained with different residue covers (15%, 35%, 55%, and 75%) for the Kostiakov, Horton, and Philip models.

The statistical indexes NSE and RMSE were used for the comparison and are shown in Table 3. The performance of the Philip model was better than the Horton model, as the lower the values of the RMSE and the closer the NSE values were to 1, the better the fitting results were. From the above, the Philip equation was optimal for the infiltration estimation of the black soil under the residue cover conditions. The equation was

$$i(t)_r = RCF_i \times (1.59 \times t^{-0.5} + 0.290), \quad (7)$$

where $i(t)_r$ is the infiltration rate under the residue cover (mm/min).

Table 3. The values of root mean square error (RMSE) and the Nash–Sutcliffe efficiency (NSE) under the Horton and Philip models.

	RMSE	NSE
Horton	0.112	0.666
Philip	0.105	0.699

4. Discussion

Four models were compared to evaluate the infiltration of black soil. The GAML model, derived from the Green–Ampt model, demonstrated that infiltration during a steady rainfall event could be simulated. However, the model was not suitable for infiltration estimations of the black soil because of the negative values observed from the hydrological parameters. It might be that the original form was usually applied to initially dry, uniform, coarse-textured soil, such as sands and sand-fraction

media [33], whereas the main textural classes of the black soil are silt clay loam and clay loam, according to the USDA (U.S. Department of Agriculture) classification [34]. As with all fine-textured soils, the resistance of soil pores to water flow was higher than in the coarse-textured soils [35]. The permeability of the black soil was poor, which caused the inapplicability of the GAML model.

The infiltration estimations of the Horton and Philip models for the residue-covered black soil performed well, with the Philip model performing better regarding the comparison of the statistical indexes NSE and RMSE. It is worth noting that both models overestimated the initial infiltration rates, especially under high residue coverage.

The average infiltration rates under the four rainfall intensities were used for the model fitting to remove the effects of heavy rain, but only the residue cover was considered, which might have been the reason for the outliers. Considering the physical significance of the Philip model, this derived residue cover infiltration model was suggested for use in estimations of cumulative infiltration amounts.

5. Conclusions

In this study, we observed the infiltration processes of black soil slopes under bare and residue-covered conditions by simulated rainfall experiments. The optimal infiltration model for the residue-covered black soil was derived in combination with the Philip model and the residue cover infiltration factor (RCF_i) after comparisons. The model was suitable for the estimation of cumulative infiltration amounts under residue cover conditions for the black soil. The model was meaningful for the infiltration estimation, and thus provided effective governance for soil erosion management of the black soil.

Author Contributions: Conceptualization, Y.X. (Yun Xie); data curation, Y.X. (Yan Xin); formal analysis, Y.X. (Yan Xin); funding acquisition, Y.X. (Yun Xie); investigation, Y.L.; methodology, Y.X. (Yan Xin) and Y.L.; supervision, Y.X. (Yun Xie); validation, Y.X. (Yan Xin); writing—original draft, Y.X. (Yan Xin); writing—review and editing, Y.X. (Yun Xie).

Funding: This work was supported by the National Key R&D Program (No. 2018YFC0507000) and the China Postdoctoral Science Foundation (No. 2018M630102).

Acknowledgments: We are thankful for the valuable comments of anonymous reviewers.

Conflicts of Interest: The authors declare no conflict of interest.

References

1. Hillel, D. *Environmental Soil Physics*; Academic Press: New York, NY, USA, 1998.
2. Zhang, J.; Lei, T.; Yin, Z.; Hu, Y.; Xiusheng Yang, X. Effects of time step length and positioning location on ring-measured infiltration rate. *Catena* **2017**, *157*, 344–356. [[CrossRef](#)]
3. Philip, J.R. Hillslope infiltration: Divergent and convergent slopes. *Water Resour. Res.* **1991**, *27*, 1035–1040. [[CrossRef](#)]
4. Herrada, M.A.; Gutiérrez-Martín, A.; Montanero, J.M. Modeling infiltration rates in a saturated/unsaturated soil under the free draining condition. *J. Hydrol.* **2014**, *515*, 10–15. [[CrossRef](#)]
5. Morbidelli, R.; Saltalippi, C.; Flammini, A.; Govindaraju, R.S. Role of slope on infiltration: A review. *J. Hydrol.* **2018**, *557*, 878–886. [[CrossRef](#)]
6. Wang, K.; Yang, X.; Liu, X.; Liu, C. A simple analytical infiltration model for short-duration rainfall. *J. Hydrol.* **2017**, *555*, 141–154. [[CrossRef](#)]
7. Green, W.; Ampt, G. Studies on soil physics, part I: The flow of air and water through soils. *J. Agric. Sci.* **1991**, *4*, 1–24.
8. Kostakov, A.N. On the dynamics of the coefficient of water percolation in soils and on the necessity of studying it from a dynamic point of view for purposes of amelioration. *Trans. Sixth Comm. Int. Soc. Soil Sci. Part A* **1932**, *1*, 7–21.
9. Horton, R. The role of infiltration in the hydrologic cycle. *Am. Geophys. Union Trans.* **1933**, *14*, 446–460. [[CrossRef](#)]

10. Holtan, H.N. *A Concept for Infiltration Estimates in Watershed Engineering*; USDA-ARS Bull. 41–51; United States Department of Agriculture, Agricultural Research Service: Washington, DC, USA, 1961.
11. Philip, J.R. The theory of infiltration: 1. The infiltration equation and its solution. *Soil Sci.* **1957**, *83*, 345–357. [[CrossRef](#)]
12. Soil Conservation Service. *SCS National Engineering Handbook*; Section 4, Hydrology; United States Department of Agriculture: Washington, DC, USA, 1972.
13. Smith, R.E.; Parlange, J.Y. A parameter-efficient hydrologic infiltration model. *Water Resour. Res.* **1978**, *14*, 533–538. [[CrossRef](#)]
14. Corradini, C.; Melone, F.; Smith, R.E. Modeling infiltration during complex rainfall sequences. *Water Resour. Res.* **1994**, *30*, 2777–2784. [[CrossRef](#)]
15. Van Den Putte, A.; Govers, G.; Leys, A.; Langhans, C.; Clymans, W.; Diels, J. Estimating the parameters of the Green–Ampt infiltration equation from rainfall simulation data: Why simpler is better. *J. Hydrol.* **2013**, *476*, 332–344. [[CrossRef](#)]
16. Mein, R.G.; Larson, C.L. Modeling infiltration during a steady rain. *Water Resour. Res.* **1973**, *9*, 384–394. [[CrossRef](#)]
17. Chu, X.; Mariño, M.A. Determination of ponding condition and infiltration into layered soils under unsteady rainfall. *J. Hydrol.* **2005**, *313*, 195–207. [[CrossRef](#)]
18. Chen, L.; Young, M.H. Green–Ampt infiltration model for sloping surfaces. *Water Resour. Res.* **2006**, *42*. [[CrossRef](#)]
19. Derpsch, R.; Franzluebbers, A.J.; Duiker, S.W.; Reicosky, D.C.; Koeller, K.; Friedrich, T.; Sturny, W.G.; Sá, J.C.M.; Weiss, K. Why do we need to standardize no-tillage research? *Soil Till. Res.* **2014**, *137*, 16–22. [[CrossRef](#)]
20. Gavin, K.; Xue, J. A simple method to analyze infiltration into unsaturated soil slopes. *Comput. Geotech.* **2008**, *35*, 223–230. [[CrossRef](#)]
21. Gong, Z.T.; Chen, Z.C.; Shi, X.Z. *Chinese Soil Taxonomy*; Science Press: Beijing, China, 1999.
22. Gu, Z.; Xie, Y.; Gao, Y.; Ren, X.; Cheng, C.; Wang, S. Quantitative assessment of soil productivity and predicted impacts of water erosion in the black soil region of northeastern China. *Sci Total Environ.* **2018**, *637*–*638*, 706–716. [[CrossRef](#)]
23. Wang, J.; Xie, Y.; Liu, G.; Zhao, Y.; Zhang, S. Soybean root development under water stress in eroded soils. *Acta Agric. Scand. Sect. B Soil Plant Sci.* **2015**, *65*, 374–382. [[CrossRef](#)]
24. Zhao, X.N.; Wu, P.; Gao, X.D.; Tian, L.; Li, H.C. Changes of soil hydraulic properties under early-stage natural vegetation recovering on the Loess Plateau of China. *Catena* **2014**, *113*, 386–391. [[CrossRef](#)]
25. Xin, Y.; Xie, Y.; Liu, Y.; Liu, H.; Ren, X. Residue cover effects on soil erosion and the infiltration in black soil under simulated rainfall experiments. *J. Hydrol.* **2016**, *543*, 651–658. [[CrossRef](#)]
26. Bamutaze, Y.; Tenywa, M.M.; Majaliwa, M.J.G.; Vanacker, V.; Bagoora, F.; Magunda, M.; Obando, J.; Wasige, J.E. Infiltration characteristics of volcanic sloping soils on Mt. Elgon, Eastern Uganda. *Catena* **2010**, *80*, 122–130. [[CrossRef](#)]
27. Nash, J.E.; Sutcliffe, J.V. River flow forecasting through conceptual models: Part 1. A discussion of principles. *J. Hydrol.* **1970**, *10*, 282–290. [[CrossRef](#)]
28. Moriasi, D.N.; Arnold, J.G.; van Liew, M.W.; Bingner, R.L.; Harmel, R.D.; Veith, T.L. Model evaluation guidelines for systematic quantification of accuracy in watershed simulations. *Trans. ASABE* **2007**, *50*, 885–900. [[CrossRef](#)]
29. Wu, L.Z.; Zhou, Y.; Sun, P.; Shi, J.S.; Liu, G.G.; Bai, L.Y. Laboratory characterization of rainfall-induced loess slope failure. *Catena* **2017**, *150*, 1–8. [[CrossRef](#)]
30. Meyer, L.D.; Wischmeier, W.H.; Foster, G.R. Mulch rates required for erosion control on steep slopes. *Soil Sci. Soc. Am. J.* **1970**, *34*, 928–931. [[CrossRef](#)]
31. Naeth, M.A.; Bailey, A.W.; Chanasyk, D.S.; Pluth, D.J. Water holding capacity of litter and soil organic matter in mixed prairie and fescue grassland ecosystems of Alberta. *J. Range Manag.* **1991**, *44*, 13–17. [[CrossRef](#)]
32. De Almeida, W.S.; Panachuki, E.; de Oliveira, P.T.S.; Da Silva Menezes, R.; Sobrinho, T.A.; de Carvalho, D.F. Effect of soil tillage and vegetal cover on soil water infiltration. *Soil Till. Res.* **2018**, *175*, 130–138. [[CrossRef](#)]
33. Mohammadzadeh-Habili, J.; Heidarpour, M. Application of the Green–Ampt model for infiltration into layered soil. *J. Hydrol.* **2015**, *527*, 824–832. [[CrossRef](#)]

34. Wu, Y.; Zheng, Q.; Zhang, Y.; Liu, B.; Cheng, H.; Wang, Y. Development of gullies and sediment production in the black soil region of northeastern China. *Geomorphology* **2008**, *101*, 683–691. [[CrossRef](#)]
35. Bouwer, H. Infiltration into increasingly permeable soils. *J. Irrig. Drain. Eng.* **1976**, *102*, 127–136.



© 2019 by the authors. Licensee MDPI, Basel, Switzerland. This article is an open access article distributed under the terms and conditions of the Creative Commons Attribution (CC BY) license (<http://creativecommons.org/licenses/by/4.0/>).